The ISME Journal (2021) 15:2379–2389
https://doi.org/10.1038/s41396-021-00938-6

ARTICLE

Iron limitation by transferrin promotes simultaneous cheating of pyoverdine and exoprotease in *Pseudomonas aeruginosa*

Oswaldo Tostado-Islas[1] · Alberto Mendoza-Ortiz[1] · Gabriel Ramírez-García[1] · Isamu Daniel Cabrera-Takane[1] · Daniel Loarca[1] · Caleb Pérez-González[1] · Ricardo Jasso-Chávez[2] · J. Guillermo Jiménez-Cortés[1] · Yuki Hoshiko[3] · Toshinari Maeda[3] · Adrian Cazares[4,5] · Rodolfo García-Contreras[1]

Received: 22 June 2020 / Revised: 29 January 2021 / Accepted: 11 February 2021 / Published online: 2 March 2021

Abstract

Pseudomonas aeruginosa is a primary bacterial model to study cooperative behaviors because it yields exoproducts such as siderophores and exoproteases that act as public goods and can be exploited by selfish nonproducers behaving as social cheaters. Iron-limited growth medium, mainly casamino acids medium supplemented with transferrin, is typically used to isolate and study nonproducer mutants of the siderophore pyoverdine. However, using a protein as the iron chelator could inadvertently select mutants unable to produce exoproteases, since these enzymes can degrade the transferrin to facilitate iron release. Here we investigated the evolutionary dynamics of pyoverdine and exoprotease production in media in which iron was limited by using either transferrin or a cation chelating resin. We show that concomitant loss of pyoverdine and exoprotease production readily develops in media containing transferrin, whereas only pyoverdine loss emerges in medium treated with the resin. Characterization of exoprotease- and pyoverdine-less mutants revealed loss in motility, different mutations, and large genome deletions (13–33 kb) including Quorum Sensing (*lasR, rsal*, and *lasI*) and flagellar genes. Our work shows that using transferrin as an iron chelator imposes simultaneous selective pressure for the loss of pyoverdine and exoprotease production. The unintended effect of transferrin uncovered by our experiments can help to inform the design of similar studies.

These authors contributed equally: Oswaldo Tostado-Islas, Alberto Mendoza-Ortiz, Gabriel Ramírez-García, Isamu Daniel Cabrera-Takane, Daniel Loarca, Caleb Pérez-González

Supplementary information The online version contains supplementary material available at https://doi.org/10.1038/s41396-021-00938-6.

✉ Adrian Cazares
acaza@ebi.ac.uk

✉ Rodolfo García-Contreras
rgarc@bq.unam.mx

[1] Departamento de Microbiología y Parasitología, Facultad de Medicina, Universidad Nacional Autónoma de México, Mexico City, Mexico

[2] Departamento de Bioquímica, Instituto Nacional de Cardiología, Mexico City, Mexico

[3] Department of Biological Functions Engineering, Kyushu Institute of Technology, Kitakyushu, Japan

[4] EMBL's European Bioinformatics Institute (EMBL-EBI), Wellcome Genome Campus, Cambridge, UK

[5] Wellcome Sanger Institute, Wellcome Genome Campus, Cambridge, UK

Introduction

Pseudomonas aeruginosa is a central bacterial model to study cooperative behaviors since it produces various exoproducts, such as siderophores, which are considered public goods [1]. Siderophores are important iron scavenging agents, essential for iron acquisition in iron-limited media; however, its production is susceptible to exploitation by social cheaters, since these molecules are released to the environment and can benefit both producer and nonproducer individuals. Most of the published works aiming to study siderophore cheating in *P. aeruginosa* have used casamino acids (CAA) medium supplemented with 100 µg/mL of human apo-transferrin (CAA TF) as iron chelator to make growth and iron acquisition dependent on siderophore production [2–7]. This medium was originally proposed by Griffin and coworkers in 2004. In 2017, Harrison and collaborators compiled a list of published experiments on siderophore cheating in *P. aeruginosa* to that date, covering 23 articles and 36 experiments, of which 32 were performed in CAA TF [2]. The list of experiments conducted in CAA

TF includes studies on the long-term coevolution between cheaters and cooperators [3], pyoverdine cheating and cheating resistance in isolates from soil and ponds [5], and the dynamics of exoprotease nonproducers and pyoverdine nonproducers in media with protein as sole carbon source and under iron limitation [8].

More recently, the use of CAA TF medium has been reported in research addressing the role of transposable phages in the evolution of social strategies in iron-limiting conditions [9], the effect of cheating in the diversity of pyoverdine variants [4], and the impact of nutrient availability in the dynamics of wild-type and siderophore nonproducer mutants [4].

The CAA TF medium has been used assuming it creates conditions specifically suitable for selecting siderophore nonproducers. Nevertheless, it is well known that quorum sensing (QS) dependent exoproteases such as elastase LasB and alkaline protease AprA greatly enhance the rate of iron acquisition through pyoverdine both in vitro and in vivo [10, 11]. Hence, during infections, iron acquisition may depend on both siderophore production and exoproteases activity, a feature that has rarely been considered in studies of pyoverdine production dynamics in vitro. Exoproteases are also public goods, and therefore susceptible to exploitation by nonproducers [12–16].

In most studies of pyoverdine production dynamics, iron in the medium has been depleted by the action of apo-transferrin, a protein susceptible to degradation by *P. aeruginosa* QS-regulated exoproteases. We therefore hypothesized that iron acquisition in such conditions is mediated by two types of public goods: siderophores (pyoverdine), and QS-regulated exoproteases that facilitate iron release by degrading apo-transferrin. Consequently, the production of both pyoverdine and exoproteases would be susceptible to being cheated by nonproducers, favoring these mutants' selection. Here we show that limiting iron availability by transferrin (TF) promotes a strong selection of exoprotease nonproducers in addition to pyoverdine-less mutants. Our experiments identified different phenotypes emerging from continuous growth in CAA TF medium in terms of pyoverdine and exoprotease production, but double cheaters of these exoproducts were prevalent at the end of the evolution experiments. Whole-genome sequencing analysis of three mutant types emerging in the experiments allowed the detection of small sequence variants associated with loss of pyoverdine production and uncovered extensive genome deletions in the exoprotease nonproducers. The deletions included QS genes, essential to produce exoproteases, as well as genes encoding diverse functions such as flagellum components. Hence, the use of transferrin as iron chelator in our experimental settings drove the emergence of exoprotease-less individuals through large genomic rearrangements affecting phenotypes other than siderophore production, an unintended effect that might have influenced similar studies.

Methods

Strains media and growth conditions

The strains used in this work and their characteristics are summarized in Table 1.

Bacteria were cultured in CAA medium (5 g casamino acids, 1.18 g K2HPO4.3H2O, 0.25 g MgSO4.7H2O and 25 mM HEPES buffer per liter), CAA TF medium (CAA medium supplemented with 20 mM $NaHCO_3$ and 100 µg/mL of human apo-transferrin), CAA chelex medium (CAA

Table 1 Strains used in this work.

Strain	Characteristics	Origin
PA14	Wild-type strain, pyoverdine, and exoprotease producer	[38]
PA14 *lasR*	PA14 with *lasR* interrupted by a transposon	[38]
CH1	PA14 isolated from CAA TF, non-pyoverdine, and non-exoprotease producer	This work
CH2	PA14 isolated from CAA chelex, non-pyoverdine producer but exoprotease producer	This work
CH3	PA14 isolated from CAA TF, pyoverdine producer and non-exoprotease producer	This work
WT1	PA14 isolated from CAA TF, pyoverdine producer, and exoprotease producer	This work
CH1-pUCP20	CH1 complemented pUCP20 plasmid	This work
CH1-*lasR*	CH1 complemented with pUCP20-*lasR*	This work
CH3-pUCP20	CH3 complemented pUCP20 plasmid	This work
CH3-*lasR*	CH3 complemented with pUCP20-*lasR*	This work
CH2-pUCP20	CH2 complemented pUCP20 plasmid	This work
CH2-*pvdS*	CH3 complemented with pUCP20-*pvdS*	This work
PA01	Wild-type strain, pyoverdine, and exoprotease producer	[39]

treated with chelex 100 resin according to the manufacturer instructions, 5 g of resin per 100 mL of medium), minimal succinate medium (MSM; 6 g K_2HPO_4, 3 g KH_2PO_4, 1 g $(NH_4)_2SO_4$, 0.2 g $MgSO_4{\cdot}7H_2O$, and 4 g succinic acid, per liter), or MSM TF medium (MSM supplemented with 20 mM $NaHCO_3$ and 100 µg/mL of human apo-transferrin). The final pH was adjusted to 7.0.

Bacteria were cultured in Erlenmeyer flasks of 50 mL of capacity filled with 5 mL of medium, and incubated at 37 °C with 200 rpm orbital shaking during 18 h for growth determination experiments and 24 h for each subculture of the evolution experiments. Each new culture was initiated with enough bacteria to reach an O.D. 600 nm of 0.05.

Isolation of pyoverdine and exoprotease-less individuals

Single colonies from the evolution experiments were obtained by streaking each subculture made in an even day on LB plates that were then incubated at 37 °C for 18 h. Around 20–50 colonies from the LB plates were subsequently passed onto King A plates and incubated under the same conditions. Green colonies displaying fluorescence under UV light were considered pyoverdine producers. Colonies from LB plates were also passed onto M9 minimal medium plates with casamino acids (0.025%) and casein (0.5%) incubated under the same conditions. Colonies producing a clear halo indicative of casein degradation were considered exoprotease producers. Three single colonies exhibiting different phenotypes were picked, grown in liquid CAA medium, and stored in 16% glycerol at −70 °C for further experiments.

Bacterial competitions

To assess the cheating capacity of some of the bacterial isolates identified as pyoverdine and/or exoprotease non-producers, they were cultured in CAA, CAA TF, and M9 Casein medium in co-culture with the wild-type strain PA14. Co-cultures were set with a 15–20% initial proportion of nonproducers and incubated during 24 h. Samples of the co-cultures were taken at the start and endpoint of the experiment and colonies were subsequently isolated for phenotypic determination (pyoverdine and exoprotease production) to calculate the strains initial and final proportions.

Iron determination

Fe content in the growth media was determined by digesting 5 mL of each medium with 5 mL of concentrated nitric acid with overnight incubation at 90 °C. The content of metals was determined by atomic absorbance spectrometry (ASS) using a Varian apparatus as previously reported [17].

Pyoverdine, exoprotease, and pyocyanin measurements

Pyoverdine in the supernatants of bacterial cultures was measured fluorometrically, using a Perkin Elmer Victor Nivo plate reader, exciting at 405 nm and recording at 510 nm [17].

Exoprotease activity was determined from culture supernatants by measuring hydrolysis of Azo-casein (SIGMA, St Louis Mo, USA) as described in [15], also using a Perkin Elmer Victor Nivo plate reader recording absorbance at 415 nm.

Pyocyanin was extracted from culture supernatants using chloroform, re-extracted with HCL 0.2 N, and measured spectrophotometrically as previously described [18].

Swimming motility assays

Plates to assess swimming motility were made with 0.25% (W/V) LB agar. After solidification, plates were dried at room temperature for 2 h. 2.5 µL aliquots taken directly from overnight LB cultures were then spotted in the center of the plates. Inoculated plates were incubated at 37 °C for 18–20 h. Motility was assessed visually after incubation.

Whole-genome sequencing and variant calling analysis

The genomic DNA used for sequencing was extracted from overnight cultures. Library synthesis was performed using the Nextera XT DNA Sample Prep Kit (Illumina, San Diego CA, USA) according to the manufacturer's instructions. TruSeq HT adapters (Illumina, San Diego CA, USA) were used to barcode the libraries, and each library was sequenced using an Illumina MiSeq 300 bp paired-end instrument. Trimmomatic v.0.39 [19] was used to process the raw fastq files for adapters removal and quality trimming with the following settings: "LEADING:3, TRAILING:3, SLIDINGWINDOW:4:23 MINLEN:35".

Single nucleotide polymorphisms (SNPs) and small indels were detected with the Snippy v3.2 pipeline (https://github.com/tseemann/snippy) by aligning the sequencing reads to the genome of the reference strain UCBPP-PA14 (Accession: NC_008463.1) with BWA-MEM [20], calling variants with FreeBayes [21], and annotating them with snpEffm [22]. The coverage metrics of the genes *lasR* and *pvdS* were determined with samtools v.1.7 [23]. Deletions flanking the *lasR* gene were inferred from coverage distribution data obtained with BEDTools [24] and identified as the longest stretch of gene coding regions featuring zero

mapped reads. De novo assembly of the genomes was carried out using SPAdes v.3.10.1 [25] with default settings. Visualization of coverage distribution and inspection of the joining regions was performed with Artemis [26]. The genome assemblies are publicly available from the Bio-Project PRJNA540579.

Complementation of the strains

The construction pUCP20-*lasR* was donated by Professor Gloria Soberón Chavez from the Institute of Biomedical Research at UNAM. For the pUCP20-*pvdS* construction, the *pvdS* gene cloned was amplified by PCR from PA14 genomic DNA. Standard methods were used to isolate the chromosomal DNA [27]. DNA restriction enzymes were purchased from New England Biolabs (NEB, Ipswich MA, USA) and the T4 DNA ligase from Invitrogen (Waltham MA, USA). Plasmid DNA was purified using an E.Z.N.A Plasmid mini kit I, (Q-spin) (Omega Bio-Tek Norcross GA, USA). The *pvdS* DNA was amplified with the oligonucleotides *pvdS*-Fw: 5′ GCTCTAGAGCCAGCATGCGGA CCATTCAC 3′ and *pvdS*-Rv: 5′ GCGAATTCACCG GCGCTGAGGAATGC 3′, using the Phusion High-Fidelity DNA polymerase (Thermo scientific, Sweden) according to the manufacturer's recommendations. The resulting *pvdS* amplicon (742 bp long including the coding region (564 bp) plus 151 upstream and 27 downstream bases) was purified with the E.Z.N.A. Cycle pure kit (Omega Bio-Tek Norcross GA, USA) and cloned into pUCP20 as a XbaI-EcoRI fragment. The constructs were transformed in to *P. aeruginosa* as indicated below. Complementation of the *lasR*-less phenotype was done in the presence and absence of 5 µM 3-Oxo-C_{12}-HSL (Sigma). Pyoverdine, caseinolytic activity and pyocyanin were determined as described above.

Transformation of *Pseudomonas aeruginosa* by $CaCl_2$

P. aeruginosa was grown overnight in LB medium with orbital shaking (200 rpm) at 37 °C. 250 µL of the cells culture were harvested by centrifugation at 15,000 × *g* for 1 min, and the pellet washed in the same volume of cold sterile Milli-Q water. The cell suspension was then centrifuged at 15,000 × *g* for 1 min and the supernatant was discarded. The cell pellet was suspended in 250 µL of 0.1 mM $CaCl_2$ and incubated for 20 min at 4 °C. The cells were subsequently centrifuged at 15,000 × *g* for 1 min, the supernatant was discarded and the cell pellet resuspended in 100 µl of 0.1 mM $CaCl_2$ with 100 ng of the pUCP20-*pvdS* or pUCP20-*lasR* construction or the empty plasmid. The suspension was maintained at 4 °C for 1 h. Cells were heat pulsed at 42 °C for 2 min by partially immersing in water and the cells suspension was incubated at 4 °C for 2 min afterwards. 500 µL of LB medium was added to the cells and then incubated at 37 °C for 1 h. Transfromed colonies were selected on King-B plates [28] containing 300 µg/mL carbenicillin.

PCRs for the confirmation of deletions

The following PCR reactions were performed to assess the presence of genomic deletions: (a) amplification of a 742 bp fragment including the gene *pvdS* as a positive control to confirm the integrity of the chromosomal DNA, using the primers *pvdS*-Fw and *pvdS*-Rv (see sequences above), (b) amplification of a fragment containing 720 bp of the gene *lasR*, using the primers F-*lasR* 5′ ATGGCCTTGGTT-GACGGTT 3′ and R-*lasR* 5′ GCAAGATCAGA-GAGTAATAAGACCCA 3′. All PCR reactions were done as previously described [29].

Statistical analysis

Results plotted in the charts are the average of at least three independent experiments ± SD or SEM. The data were analyzed using the IBM SPSS Statistics software and the statistical tests Mann–Whitney, Kruskall–Wallis and Student *T*-test were applied as specified in the figure legends of the different plots. Differences were considered significant when *P* values were lower than 0.05.

Results

Selection of siderophore and exoprotease nonproducers in the presence of apo-transferrin

To explore the impact of transferrin on exoprotease production, colonies of the *P. aeruginosa* strain PA14 were grown and serially transferred in CAA medium supplemented with apo-transferrin (CAA TF) for 14 serial passages and periodically tested for pyoverdine and exoprotease production. Siderophore-less mutants were identified from passage number 6 (~24 generations). Figure 1a shows that in parallel to selection of pyoverdine-less mutants, there was a strong selection of exoprotease nonproducers. A screening of single colonies of the two phenotypes revealed that most of them exhibit concomitant loss of pyoverdine and exoproteases production (Fig. S1).

To test whether the presence of apo-transferrin was responsible for selecting exoprotease-less mutants, a new set of experiments was done in CAA medium using the chelex 100 resin as the iron-depletion factor. Non-treated CAA and MSM were also used as a control and as an alternative of iron-limited medium, respectively. Our results show that pyoverdine nonproducers appeared from passage 6 (Fig. 1a, b) and were selected upon passage 14 in all

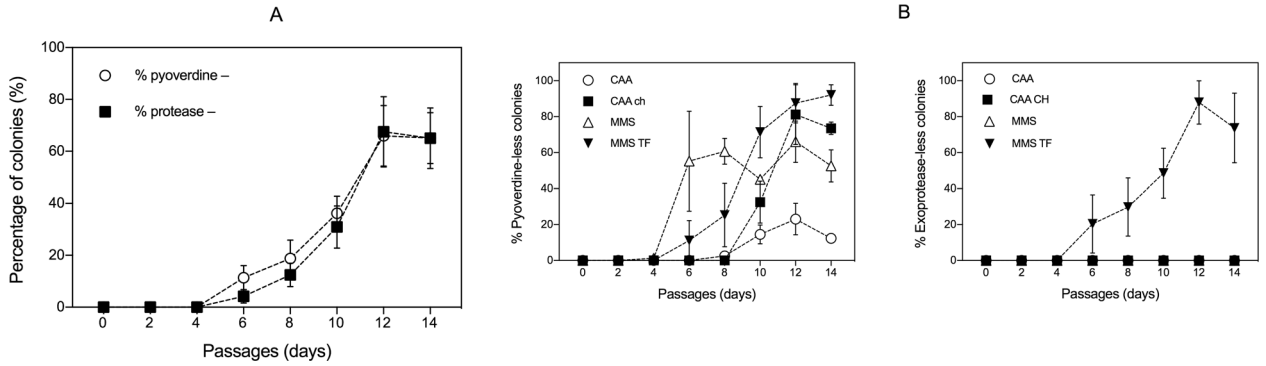

Fig. 1 Selection of non-protease and non-siderophore producers in different culture media. A Percentage of pyoverdine and exoprotease nonproducers of the PA14 strain identified during sequential subculture in CAA medium supplemented with transferrin (CAA TF). Results are the average of eight independent experiments ± SEM. No significant differences between the percentages of non-pyoverdine and non-protease producers were found using a Mann–Whitney *U* test. **B** Percentage of pyoverdine (left) and exoproteases (right) nonproducers of the strain PA14 identified during sequential subculture in CAA medium, CAA medium treated with chelex 100 (CAA ch), minimal succinate medium (MMS), and minimal succinate medium supplemented with transferrin (MMS TF). Results are the average of three independent experiments ± SEM.

media. These mutants were more abundant in the CAA medium treated with chelex, and in MMS, than in the non-treated CAA medium (Fig. 1b), as expected from the level of iron availability in those media (13.1 ± 3.25, 7.12 ± 1.8, and 66.3 ± 24.7 μM for CAA chelex, MMS, and CAA respectively). We did not find exoprotease nonproducers during the screening of bacteria grown in media lacking apo-transferrin (Fig. 1b). In contrast, adding apo-transferrin to the MSM promoted selection of exoprotease-less mutants in parallel to pyoverdine nonproducers (Fig. 1b), thus confirming that presence of apo-transferrin imposes a selective pressure for the loss of exoprotease production. The addition of TF to the CAA medium also promoted the emergence of exoprotease and pyoverdine-less individuals in sequential cultures of the reference strain PA01 (Fig. S2), indicating that this effect is not exclusive to the strain PA14.

Characterization of pyoverdine and exoprotease nonproducer individuals

Our experiments demonstrated that the CAA TF medium selects the loss of both pyoverdine and exopreotease production. Hence, four different types of individuals are expected to occur in the population: wild-type (wt, pyoverdine, and exoprotease producers), pyoverdine cheaters (pyoverdine nonproducer, exoprotease producers), exoprotease cheaters (pyoverdine producer, exoprotease nonproducers), and double cheaters (pyoverdine and exoprotease nonproducers). We confirmed the presence of the four types of individuals in the experiment in CAA TF medium and recorded their frequency from passage 6 to 14. Double cheaters were the predominant cheater type from passage 8 and reached around 90% of the population in passage 14 (Fig. S1), suggesting that these individuals have greater fitness than those losing a single trait.

Next, we characterized a set of individual colonies by measuring production of pyoverdine and exoproteases (caseinolytic activity), and growth in different media. The selected colonies were representative of the three different cheater phenotypes identified in the experiment: pyoverdine and exoprotease nonproducer (CH1), pyoverdine producer but exoprotease nonproducer (CH3), and pyoverdine non-producer but exoprotease producer (CH2). We found that growth of the three isolates was similar to PA14 wild-type in CAA medium; however, the pyoverdine nonproducers (CH1 and CH2) grew less than the wild-type strain in iron-limited media (CAA TF and CAA chelex) (Fig. S3). Likewise, exoprotease nonproducers (CH1 and CH3) grew less than the wild-type strain in the medium containing casein as sole carbon source (Fig. S3). As expected, the levels of fluorescence in the pyoverdine nonproducers CH1 and CH2 were lower than in the CH3 isolate (Fig. 2a). The caseinolytic activity assay also confirmed the reduction in exoprotease activity in CH1 and CH3 but not in the CH2 strain (Fig. 2b). Competition experiments between PA14 wild-type and two different CH strains showed that CH1 can cheat both pyoverdine and exoprotease since its frequency in co-cultures increased after 24 h in CAA TF and M9 Casein media but not in non-treated CAA medium (Fig. 3a), whilst CH2 increased its frequency only in an iron-limiting condition (Fig. 3b).

Whole-genome sequencing

To get insights into the genetic basis of the loss of exoprotease and pyoverdine production, we performed whole-genome sequencing of the PA14 wild-type strain used in this work, the three CH isolates, and an additional clone with wild-type phenotype isolated from the CAA-TF experiments (WT1). A variant calling analysis targeting small indels and

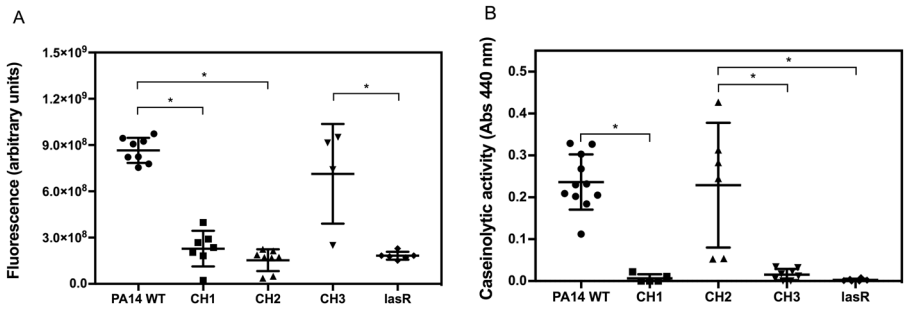

Fig. 2 Pyoverdine and exoprotease production of selected clones. **A** Pyoverdine production of the PA14 wild-type strain, three PA14-derived isolates from the evolution experiments (CH1, CH2, CH3), and a *lasR* deletion mutant. Plotted are the individual values of at least four independent experiments, and the averages ± SEM. Significant differences in production of pyoverdine between PA14 WT and CH1 ($p = 0.023$), PA14 WT and CH2 ($p = 0.001$), CH2 and CH3 ($p = 0.019$), and PA14 WT and *lasR* ($p = 0.005$) were found using a Krustall–Wallis test ($p < 0.001$) with Bonferroni correction. **B** Exoprotease production (caseinolitic activity) of the PA14 wild-type strain, three PA14-derived isolates from the evolution experiments (CH1, CH2, CH3), and a *lasR* deletion mutant. The values plotted correspond to the individual values and the average of at least five independent experiments ± SEM. Significant differences in exoprotease production between PA14 WT and CH1 ($p = 0.005$), PA14 WT and CH3 ($p = 0.002$), CH1 and CH2 ($p = 0.015$), CH2 and *lasR* ($p = 0.007$), and PA14 WT and *lasR* ($p = 0.002$) were found using a Krustall–Wallis test ($p < 0.001$) with Bonferroni correction.

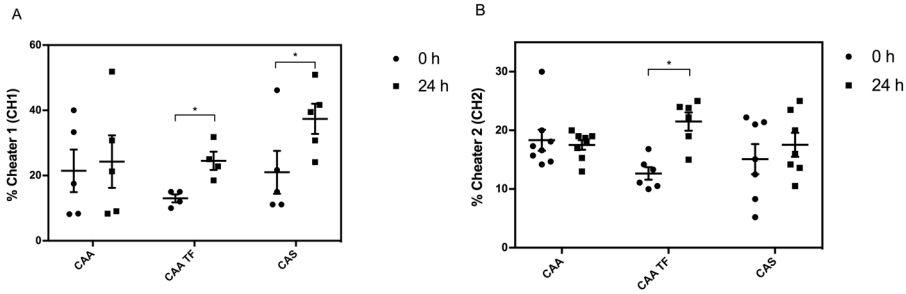

Fig. 3 Competitions between the wild-type and evolved strains in diferent media. Competitions between the PA14 wild-type strain and CH1 (**A**) or CH3 (**B**) in CAA medium, CAA medium supplemented with transferrin (CAA TF), and caseinate medium (CAS). The bar plots show the individual values and the average ± SD of the initial (circles) and after 24 h (squares) proportion of CH1 in the competition experiments. The experiments were performed in triplicate. The differences between the initial and after 24 h proportions of CH1 in CAA TF and CAS media are significant according to *T*-test, $P > 0.05$. Also, the differences between proportions of CH3 are significant in CAA TF medium.

SNPs identified few mutations occurring in the CH isolates but not in the wild-type and WT1 strains (Supplementary Table 1). Multiple reports [3, 9, 14, 15, 30] have linked punctual mutations in the genes *pvdS* and *lasR* to loss of pyoverdine and exoprotease production, respectively. We identified a frameshift mutation in the gene *pvdA* and one mutation in the intergenic region upstream the gene *pvdS* in the genomes of the pyoverdine nonproducer isolates CH1 and CH2, respectively. However, no mutations with a clear association with loss of exoprotease production were detected in the nonproducer strains CH1 and CH3. We did not identify other small variant in CH1 besides the mutation in *pvdA*, whereas CH3 featured mutations in a couple of genes encoding hypothetical proteins. To assess whether low sequencing coverage hampered the identification of mutations in the regions encoding LasR and PvdS, we determined the coverage metrics for these genes in all the isolates (Supplementary Table 1). Hundreds of reads covered the *pvdS* coding sequence in all the genomes with comparable RPKM values. In contrast, very few or no reads mapping *lasR* were detected in the genomes of the exoprotease nonproducers CH1 and CH3. Detailed examination of the *lasR*-flanking regions in both genomes revealed several genes with zero reads coverage, indicative of large deletions (Fig. 4). The coverage assessment of the regions predicted the loss of ~33 and 13 kb in the CH1 and CH3 genomes, respectively (Fig. 4). The putative deletions included flagellar genes, components of an RND multidrug efflux pump, and the quorum-sensing genes *lasI*, *rsaL*, and *lasR* (entirely or partially) (Supplementary Table 1). Additionally, the deletion in CH1 covered some transporters, regulators, and a larger number of flagellar genes, among others.

Confirmation of genome deletions and motility tests

We designed primers targeting the genes *lasR* and *pvdS* to validate the deletions identified in the CH1 and CH3 isolates. The fragment corresponding to the amplification of *lasR* was detected in CH2 and wild-type strains but not in CH1 and CH3 (Fig. S4). Conversely, *pvdS* was amplified in all the strains, as anticipated from our genome analysis. Since deletions in CH1 and CH3 include several flagellar genes, we further assessed the functional impact of this genomic loss by evaluating the isolates' swimming motility. Neither CH1 nor CH3 exhibited motility, in contrast to the wild-type and CH2 strains which lack the genome deletion (Fig. S5).

Next, we assembled the CH1 and CH3 genomes to identify the newly generated joining regions and better define the deletions' structure. Contigs containing junctions between the regions flanking the deletions were recognized in the two genomes (Fig. 5). Detailed examination of the junctions revealed that in CH1 the deletion removed 33.2 kb of the genome, including 30 coding regions and a portion of the genes *flhB* and RS18715 where the chromosome breaks occurred. In CH3, the intergenic region between *fliL* and *fliK*, and the gene *lasR*, correspond to the chromosome

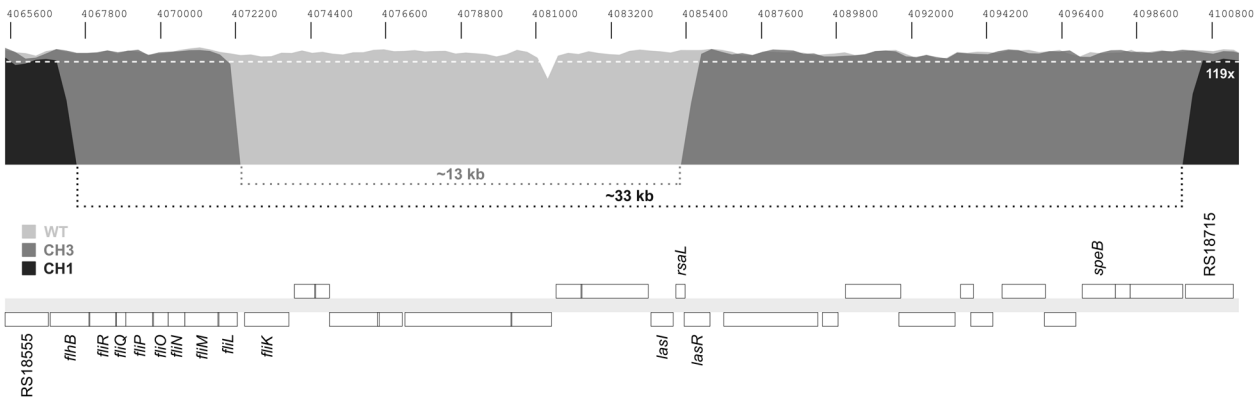

Fig. 4 Multigene deletions on the genomes of the isolates CH1 and CH2. The figure shows the coverage distribution of sequencing reads mapping a selected region of the PA14 genome (NC_008463). Coordinates of the selected region are displayed above the sequencing coverage plot. Coverage by reads from the CH1, CH2, or wild-type (WT) genomes is color coded and indicated in the figure. A white dotted line in the plot indicates a reference coverage value. The position and approximate length of regions featuring zero mapped reads from the CH1 and CH2 genomes, indicative of deletions, is marked by dotted lines below the coverage plot. A gene map of the PA14 selected region is shown at the bottom of the figure with genes represented by white boxes. Names or locus tags of genes of interest are indicated above or below their corresponding boxes.

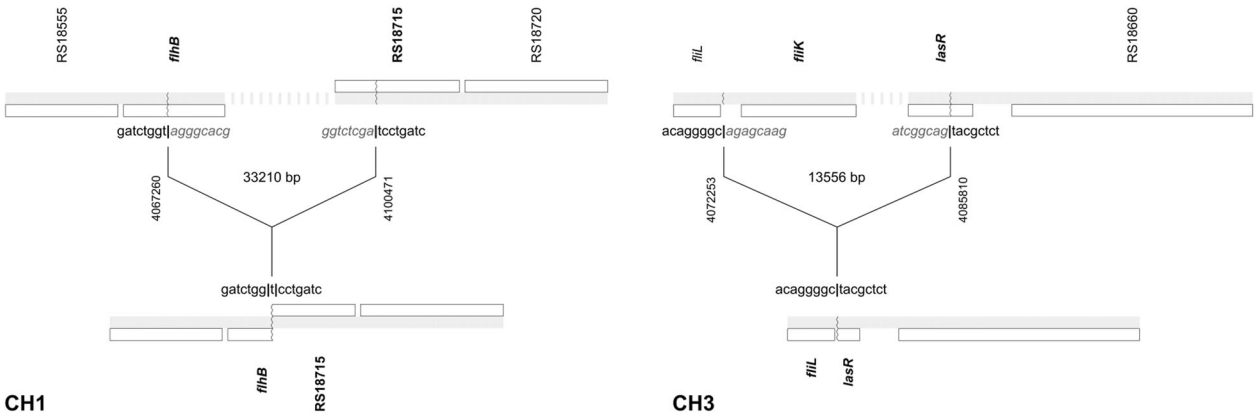

Fig. 5 Junctions between regions flanking multigene deletions in the CH1 and CH3 genomes. Diagrams in the figure illustrate the chromosome breaks (top) and joining regions (bottom) of deletions identified in the genomes of the CH1 (left) and CH3 (right) isolates. Gene maps in the diagrams are draw to scale according to the annotations and coordinates of the PA14 genome (NC_008463). Genes are represented by white boxes. Gene names or locus tags are shown next to their corresponding boxes. The deletion breakpoints in the chromosome are depicted as zigzag lines in the maps and the genes affected by them are marked in bold typeface. The nucleotide sequences flanking the breakpoints prior deletion (top) and after junction (bottom), are presented in the figure. The position of the breakpoints prior deletion is indicated at the center of the diagrams along with the length of the deletion. The joining regions displayed in the figure were identified in contigs resulting from the assembly of the CH1 and CH3 genomes.

breakpoints of the 13.5 kb deletion that removed 11 genes and 157 of the 240 codons in *lasR*. In CH1 the chromosome breaks rejoin merging the *flhB* and RS18715 coding sequences, whereas in CH3 the junction modifies and shortens the *lasR* sequence by introducing seven new amino acids and a premature stop codon (Fig. 5). It is unclear, however, whether any of the coding sequences disrupted by deletions in CH1 and CH3 can still generate a protein.

Complementation of cheater phenotypes

Our genome sequence analysis revealed large deletions encompassing the Quorum-sensing (QS) genes *lasI* and *lasR* (partially or entirely) in the strains CH1 and CH3. Multiple studies on exoprotease cheating report that non-producers selected in medium containing protein as sole carbon source are commonly characterized as *lasR*-less mutants. Since the isolates carrying genome deletions lack *lasI*, we hypothesized that loss of exoprotease production could be complemented by an exogenous *lasR* only with the addition of the 3-Oxo-C_{12}-HSL signal. Consistent with this notion, transformation of CH3 with the construction pUCP20-*lasR* led to recovering exoprotease production only in the presence of 3-Oxo-C_{12}-HSL in the medium (Fig. S6A). Pyocyanin production, also dependent on functional QS, was measured in the CH3 strain carrying pUCP20-*lasR*, with and without the addition of the 3-Oxo-C_{12}-HSL signal. The results showed that CH3 is deficient in pyocyanin production, which can be complemented with pUCP20-*lasR* only when the signal is added (Fig. S6A). Likewise, CH1 recovered exoprotease production in the presence of pUCP20-*lasR* and 3-Oxo-C_{12}-HSL (Fig. S6B). We also tested whether the CH2 isolate (pyoverdine non-producer, exoprotease producer) was defective due to lack of expression of the sigma factor *pvdS*, finding that complementation with an exogenous *pvdS* largely alleviates its deficit in pyoverdine production (Fig. S6C).

Analysis of additional clones

To further explore the presence of deletion mutants in the evolution experiments, we analyzed 47 additional clones recovered from serial passages of PA14 and PA01 in CAA TF or CAA chelex. Since CH strains featuring genome deletions were nonmotile, lacked multiple flagellar genes and a complete *lasR* gene, the new set of isolates was tested for motility and presence of *lasR* as proxy for identification of the deletion. Presence of the gene *pvdS* was tested as a positive control in the PCR. Moreover, characterization of the 47 isolates included determination of pyoverdine and exoprotease production.

The analysis uncovered a diversity of phenotypes and genotypes in the PA14 and PAO1 populations, including those observed in the previously characterized CH strains (Supplementary Table 2). Clones losing pyoverdine and exoprotease production were common, arose from both PA14 and PAO1 cultures, and were observed in CAA TF but not CAA chelex. Most of these clones (12 out of 15) were nonmotile and lacked amplification of the *lasR* gene, implying the occurrence of a deletion similar to those identified in the CH1 and CH3 strains. In contrast, clones with wild-type phenotype were motile and amplified *lasR*. Importantly, mutants impaired in exoprotease production, either solely or in combination with pyoverdine loss, were only observed in CAA TF, implicating transferrin as a key factor in the emergence of this trait. In most cases, exoprotease nonproducers featured putative deletions including the gene *lasR*.

Discussion

Siderophore cheating has been extensively studied in the laboratory using *P. aeruginosa* as the main model because it represents an important and frequent behavior in bacterial communities [31]. Lack of pyoverdine production is widespread among *P. aeruginosa* clinical isolates from cystic fibrosis patients. Furthermore, the occurrence of these strains, which retain the ability to uptake iron becoming potential cheaters in the population, increases with colonization time. Similarly, *P. aeruginosa* QS-deficient mutants unable to produce exoproteases are commonly isolated from infections [32], in coexistence with QS-proficient isolates [33]. Loss of public goods production and cheating thus seems to be a frequent phenomenon in *P. aeruginosa* and may contribute to attenuate its virulence during chronic infections. In fact, inoculating social cheaters in infections has been proposed as a strategy to attenuate host damage [34], supported by experimental evidence from animal infection models [35].

The strong selection for loss of exoprotease production upon cultivation with apo-transferrin presented here suggests that iron acquisition in similar experimental conditions not only depends on pyoverdine production, as initially assumed. In line with previous reports [10], our data suggests that the activity of exoproteases breaking down transferrin and facilitating release of the iron bound to it enhances iron acquisition through pyoverdine. Since both siderophores and exoproteases are public goods, mutants that lose the expression of one or both traits benefit from the production of these factors by cooperator individuals in the population, thus exploiting them. Correspondingly, emergence and selection of different pyoverdine and exoprotease mutants was observed in our evolution experiments in medium supplemented with apo-transferrin.

Our genome analyses revealed that loss of exoprotease production in the CH1 and CH3 mutants is not driven by punctual mutations in *lasR*, but by extensive genome deletions including the *lasR* and *lasI* genes. Accordingly, complementation of exoprotease production in these mutants was achieved by an exogenous *lasR* in the presence of 3-Oxo-C_{12}-HSL (Fig. S4A, B). A cluster of flagellar genes was also included in the deletions detected in CH1 and CH3, consistent with the lack of swimming motility detected in these exoprotease-less mutants. In the strain CH2, loss of pyoverdine production was complemented by an exogenous *pvdS*, in agreement with the mutation identified in the putative promoter region of this gene. Similar mutations affecting *pvdS* have been found in other studies [3].

Characterization of various clones from the evolution experiments revealed that mutants deficient in exoprotease production readily emerge in CAA TF and typically exhibit concomitant loss of pyoverdine production (Supplementary Table 2). Exoprotease nonproducers arose in PAO1 and PA14 cultures, indicating that these individuals' occurrence in the population is strain independent. As observed with the strains CH1 and CH3, most of the exoprotease nonproducers were nonmotile and did not amplify the *lasR* gene, implying that genome deletions including QS and flagellar genes are commonly linked to exoprotease loss in these experimental conditions. Similarly, mutations in motility and QS genes, and a 6.6 kb deletion affecting pyoverdine biosynthesis genes, were reported in the strain PAO6609; a *P. aeruginosa* mutant recurrently used as a cheat strain in the study of siderophore cooperation [2]. These findings suggest that losing QS and likely exoproteases production may be favorable for cheating in this mutant and that deletions could also be responsible for pyoverdine loss. Intriguingly, no deletion targeting *lasIR* was reported in the study by Kummerli et al. [3]. We sought to assess the presence of deletions affecting this or other genes in the genomes reported in this work; however, the raw sequencing data was not available from public databases. Altogether, the observations on the occurrence and impact of deletions in these systems are remarkable since this type of genome rearrangement is typically neglected during the analysis of experimental evolution sequencing data and can impact various significant phenotypes. Therefore, we encourage authors to analyze or revisiting their sequencing data, considering the occurrence of large genome deletions.

Diverse phenotypes and genotypes were identified among the additional clones retrieved from the evolution experiments (Supplementary Table 2). Several corresponded to those recognized in the three CH strains; however, other strain types were also detected. For example, exoprotease nonproducers amplifying the gene *lasR* were identified, although in some instances producing an amplicon of size lower than expected, suggestive of a deletion within the *lasR* coding region. These strains appeared to be less frequent than those featuring putative large deletions; nevertheless, their presence hints alternative ways of driving exoprotease loss during serial culturing in CAA TF. Further genome characterization will be necessary to reveal the genetic basis of exprotease loss in these isolates and identify the broad spectrum of genome variation arising in similar iron-limiting conditions in vitro and in vivo.

The lack of motility developed in some of our isolates is in line with previous findings reporting the inactivation of flagellar genes through punctual mutations in both pyoverdine nonproducers and cooperators when the PA01 strain is serially cultured in CAA TF [3] and suggests that lack of motility could be beneficial in such culture conditions. One possible explanation is that swimming does not confer an advantage during growth on shaking. Yet, the flagellum synthesis and function are energetically costly and losing it would allow the bacterium to save energy for other cellular processes.

Experimental evolution studies on the development of resistance to gallium, a group IIIa metal that can mimic iron and interfere with iron-dependent cellular functions, also involve the use of apo-transferrin to deplete iron in CAA medium. We consider that selection for loss of exoprotease production represents a key variable likely overlooked in these studies' experiments. In line with our findings, Bonchi et al. [36] reported a weak correlation between pyoverdine production and *P. aeruginosa* clinical strains' ability to grow in human serum, nevertheless, a strong correlation between growth and exoprotease production was identified. The positive correlation between growth and proteolytic activity was due to degradation of the transferrin present in the serum leading to facilitation of iron release and uptake by pyoverdine, which translated into reduced susceptibility to the inhibitory effects of gallium [36].

Recent research shows that coexistence between wild-type cells, pyoverdine and elastase nonproducer mutants is stable in low-iron conditions with casein as sole carbon source. Since the medium used in this study's experiments relies on apo-transferrin for achieving iron limitation [8], it would be interesting to test whether the same stability is observed when iron availability is limited by methods other than the utilization of iron-chelating proteins.

Others authors have reported that CAA TF does not necessarily resemble *P. aeruginosa* growth conditions in vivo [2]. Here we show that strong selection for exoprotease-less mutants promoted by sequential culturing in this medium may have been previously overlooked, and propose the utilization of other strategies for generating iron-limiting media. In our case, using iron-chelating resins removed 80% of the iron in the medium. Alternatively,

nonprotein iron chelators such as 2,2′-bipyridine have been used to study siderophore cheating in *Burkholderia cenocepacia* [37]. On the other hand, a possible disadvantage of using this type of chelating agents is that they may remove other important divalent cations, causing additional effects such as overproduction of different metal chelators. Yet, to minimize this kind of bias, relevant cations could be quantified before and after treatment, adding missing cations into the medium artenatively, a non-protease producing mutant could be used in experiments with transferrin as the iron-chelating agent. We hope that our work increase the awareness of the importance of the choice of experimental condition in experimental evolution.

Acknowledgements RG-C research is funded by CONACYT grant CB 2017-2018 number A1-S-8530 and by PAPITT UNAM grant number IN214218, we are grateful with Cecilia Martinez Castillo for her technical assistance with some experiments.

Compliance with ethical standards

Conflict of interest The authors declare no competing interests.

Publisher's note Springer Nature remains neutral with regard to jurisdictional claims in published maps and institutional affiliations.

References

1. Smith P, Schuster M. Public goods and cheating in microbes. Curr Biol. 2019;29:R442–7.
2. Harrison F, McNally A, Da Silva AC, Heeb S, Diggle SP. Optimised chronic infection models demonstrate that siderophore 'cheating' in *Pseudomonas aeruginosa* is context specific. ISME J. 2017;11:2492–509.
3. Kümmerli R, Santorelli LA, Granato ET, Dumas Z, Dobay A, Griffin AS, et al. Co-evolutionary dynamics between public good producers and cheats in the bacterium *Pseudomonas aeruginosa*. J Evol Biol. 2015;28:2264–74.
4. Stilwell P, Lowe C, Buckling A. The effect of cheats on siderophore diversity in *Pseudomonas aeruginosa*. J Evol Biol. 2018;31:1330–9.
5. Butaite E, Baumgartner M, Wyder S, Kümmerli R. Siderophore cheating and cheating resistance shape competition for iron in soil and freshwater *Pseudomonas* communities. Nat Commun. 2017;8:414.
6. Jin Z, Li J, Ni L, Zhang R, Xia A, Jin F. Conditional privatization of a public siderophore enables *Pseudomonas aeruginosa* to resist cheater invasion. Nat Commun. 2018;9:1383.
7. Leinweber A, Fredrik Inglis R, Kümmerli R. Cheating fosters species co-existence in well-mixed bacterial communities. ISME J. 2017;11:1179–88.
8. Özkaya Ö, Balbontín R, Gordo I, Xavier KB. Cheating on cheaters stabilizes cooperation in *Pseudomonas aeruginosa*. Curr Biol. 2018;28:2070–80.
9. O'Brien S, Kümmerli R, Paterson S, Winstanley C, Brockhurst MA. Transposable temperate phages promote the evolution of divergent social strategies in *Pseudomonas aeruginosa* populations. Proc R Soc B Biol Sci. 2019;286:20191794.
10. Wolz C, Hohloch K, Ocaktan A, Poole K, Evans RW, Rochel N, et al. Iron release from transferrin by pyoverdin and elastase from *Pseudomonas aeruginosa*. Infect Immun. 1994;62:4021–7.
11. Kim SJ, Park RY, Kang SM, Choi MH, Kim CM, Shin SH. *Pseudomonas aeruginosa* alkaline protease can facilitate siderophore-mediated iron-uptake via the proteolytic cleavage of transferrins. Biol Pharm Bull. 2006;29:2295–300.
12. Sandoz KM, Mitzimberg SM, Schuster M. Social cheating in *Pseudomonas aeruginosa* quorum sensing. Proc Natl Acad Sci USA. 2007;104:15876–81.
13. Diggle SP, Griffin AS, Campbell GS, West SA. Cooperation and conflict in quorum-sensing bacterial populations. Nature. 2007;450:411–4.
14. Dandekar AA, Chugani S, Greenberg EP. Bacterial quorum sensing and metabolic incentives to cooperate. Science. 2012;338:264–6.
15. Loarca D, Díaz D, Quezada H, Guzmán-Ortiz AL, Rebollar-Ruiz A, Presas AMF, et al. Seeding public goods is essential for maintaining cooperation in *Pseudomonas aeruginosa*. Front Microbiol. 2019;10:1–8.
16. García-Contreras R, Loarca D, Pérez-González C, Jiménez-Cortés JG, Gonzalez-Valdez A, Soberón-Chávez G. Rhamnolipids stabilize quorum sensing mediated cooperation in *Pseudomonas aeruginosa*. FEMS Microbiol Lett. 2020;367:1–5.
17. García-Contreras R, Lira-Silva E, Jasso-Chávez R, Hernández-González IL, Maeda T, Hashimoto T, et al. Isolation and characterization of gallium resistant *Pseudomonas aeruginosa* mutants. Int J Med Microbiol. 2013;303:574–82.
18. Castañeda-Tamez P, Ramírez-Peris J, Pérez-Velázquez J, Kuttler C, Jalalimanesh A, Saucedo-Mora M, et al. Pyocyanin restricts social cheating in *Pseudomonas aeruginosa*. Front Microbiol. 2018;9:1–10.
19. Bolger AM, Lohse M, Usadel B. Trimmomatic: A flexible trimmer for Illumina sequence data. Bioinformatics. 2014;30:2114–20.
20. Li H. Aligning sequence reads, clone sequences and assembly contigs with BWA-MEM. arXiv. 2013;00:1–3.
21. Garrison E, Marth G. Haplotype-based variant detection from short-read sequencing -- Free bayes -- Variant Calling -- Long-ranger. arXiv Prepr arXiv12073907 2012.
22. Cingolani P, Platts A, Wang LL, Coon M, Nguyen T, Wang L, et al. A program for annotating and predicting the effects of single nucleotide polymorphisms, SnpEff. Fly. 2012;6:80–92.
23. Li H, Handsaker B, Wysoker A, Fennell T, Ruan J, Homer N, et al. The Sequence Alignment/Map format and SAMtools. Bioinformatics. 2009;25:2078–9.
24. Quinlan AR, Hall IM BEDTools: A flexible suite of utilities for comparing genomic features. Bioinformatics. 2010;26:841–2.
25. Bankevich A, Nurk S, Antipov D, Gurevich AA, Dvorkin M, Kulikov AS, et al. SPAdes: A new genome assembly algorithm and its applications to single-cell sequencing. J Comput Biol. 2012;19:455–77.
26. Carver T, Harris SR, Berriman M, Parkhill J, McQuillan JA. Artemis: An integrated platform for visualization and analysis of high-throughput sequence-based experimental data. Bioinformatics. 2012;28:464–9.
27. Ausubel FM, Brent R, Kingston RE, Moore DD, Seidman JG, Smith JA, et al. Current protocols in molecular biology: preface. Curr Protoc Mol Biol. 2010;1:178–89.
28. King EO, Ward MK, Raney DE. Two simple media for the demonstration of pyocyanin and fluorescin. J Lab Clin Med. 1954;44:301–7.
29. López-Jácome LE, Garza-Ramos G, Hernández-Durán M, Franco-Cendejas R, Loarca D, Romero-Martínez D, et al. AiiM lactonase strongly reduces quorum sensing controlled virulence factors in clinical strains of *Pseudomonas aeruginosa* isolated from burned patients. Front Microbiol. 2019;10:1–11.
30. Sandoz KM, Mitzimberg SM, Schuster M. Social cheating in *Pseudomonas aeruginosa* quorum sensing. Proc Natl Acad Sci USA. 2007;104:15876–81.

31. D'Onofrio A, Crawford JM, Stewart EJ, Witt K, Gavrish E, Epstein S, et al. Siderophores from neighboring organisms promote the growth of uncultured bacteria. Chem Biol. 2010;17:254–64.
32. Wang Y, Gao L, Rao X, Wang J, Yu H, Jiang J, et al. Characterization of lasR-deficient clinical isolates of *Pseudomonas aeruginosa*. Sci Rep. 2018;8:13344.
33. Wilder CN, Allada G, Schuster M. Instantaneous within-patient diversity of *Pseudomonas aeruginosa* quorum-sensing populations from cystic fibrosis lung infections. Infect Immun. 2009;77:5631–9.
34. Brown SP, West SA, Diggle SP, Griffin AS. Social evolution in micro-organisms and a Trojan horse approach to medical intervention strategies. Philos Trans R Soc B Biol Sci. 2009;364:3157–68.
35. Rumbaugh KP, Diggle SP, Watters CM, Ross-Gillespie A, Griffin AS, West SA. Quorum sensing and the social evolution of bacterial virulence. Curr Biol. 2009;19:341–5.
36. Bonchi C, Frangipani E, Imperi F, Visca P. Pyoverdine and proteases affect the response of *Pseudomonas aeruginosa* to gallium in human serum. Antimicrob Agents Chemother. 2015;59:5641–6.
37. Sathe S, Mathew A, Agnoli K, Eberl L, Kümmerli R. Genetic architecture constrains exploitation of siderophore cooperation in the bacterium *Burkholderia cenocepacia*. Evol Lett. 2019;3:610–22.
38. Liberati NT, Urbach JM, Miyata S, Lee DG, Drenkard E, Wu G, et al. An ordered, nonredundant library of *Pseudomonas aeruginosa* strain PA14 transposon insertion mutants. Proc Natl Acad Sci USA. 2006;103:2833–8.
39. Chandler CE, Horspool AM, Hill PJ, Wozniak DJ, Schertzer JW, Rasko DA, et al. Genomic and phenotypic diversity among ten laboratory isolates of *Pseudomonas aeruginosa* PAO1. J Bacteriol. 2019;201.